IJISET - International Journal of Innovative Science, Engineering & Technology, Vol. 2 Issue 1, January 2015.
www.ijiset.com
ISSN 2348 – 7968

Resistance Based Damage Sensing in electrically Non Conductive Composites using Carbon Nanotubes

Satheesh kumar.V, Dr.Dalbir Singh, Associate Professor, Mrs Nisha.M.S, Assistant Professor
Hindustan college of Engineering and Technology, Padur, Chennai, India.

ABSTRACT

Damage sensing is defined as process of observing, measuring and reporting the damage and non conformities in a structure. It can be performed by the use of sensors that are embedded in a structure or attached on the surface of the structure. Alternately, it can be performed by using the structural material itself as the sensor. Currently emerging damage sensing approaches include the use of strain- gages, accelerometers, piezoelectric sensors and fiber optic sensors to measure strain, vibration, harmonic frequencies, or other parameters which can be used to assess the health of the structure by comparing these values to a known healthy dataset. Many of these methods provide sensing only near the sensor itself; therefore, they must be placed at or near critical regions of interest in order to detect damage. If damage occurs at other unanticipated regions, it may not detect. Embedding of the sensors are generated artificial defects that which downgrade the mechanical properties of the composite. In the present work, Poly Vinyl Alcohol (PVA) and carbon nanotube (CNT) were used to prepare nanofibers that had been embedded to glass fiber reinforced polymers (GFRP) for the damage sensing of the composite material. It does not downgrade the mechanical properties of the composite. Various incremental loading-unloading steps had been applied to test the specimens in tension as well as three-point bending tests. A direct correlation between the mechanical loading and the electrical resistance change had been established for the investigated specimens.

Key words: Glass fiber reinforced polymers, Carbon nanotube, Poly Vinyl Alcohol, Damage sensing

1. INTRODUCTION

The failure of a fiber composite is a complex process which may involve an accumulation of microscopic damage, including fiber fracture, fiber matrix interfacial debonding, matrix cracking and delamination. The concept of damage sensing in composites based upon the carbon fiber reinforcements was used by Schulte [1]. The basic idea of this approach is in the use of conductive carbon fibers as the electric current carrier and the measurement of resistivity change in the fiber direction due to fiber breakages or in the transverse direction due to the separation of fiber contacts [2, 3]. However, the technique is not applicable to composites with non-conductive fibers such as glass and ceramic fibers. Even in carbon fiber composites, some matrix-dominated damage may not be detected by the fiber network. Thus, more versatile technique is needed for in situ damage sensing of fiber-reinforced composites, and carbon nanotubes (CNTs) turn out to have great potential for such applications [4,5].

Carbon nanotubes (CNT) are known as the stiffest and strongest materials in the world. They were discovered in the early 1990s and researchers started to focus on

these new materials due to their considerable physical and mechanical properties. Their remarkable mechanical properties such as high stiffness and strength, exceptional resilience, low density, fiber-like structure with high aspect ratio (length/diameter), as well as high electrical and thermal conductivity render carbon nanotubes (CNTs) potential as nanoscaled reinforcement to achieve improved electrical properties [6]. Recently, researchers have utilized them as strain sensors by embedding them in polymer matrix composites (PMCs) and monitoring damage and subsequently failure, by direct measurement of current in the composite [7].

Wichmann et al [7] were proposed the concept of conductive modification with nanotubes for both strain and damage sensing. Because CNTs possess higher electrical conductivity than carbon fibers, it is expected that the sensitivity of changes in electrical resistance resulted from strain or damage could be enhanced. Thostenson and Chou [8] concluded that the change in the size of reinforcements, from conventional micron-sized fiber reinforcement to carbon nanotubes with nanometer-level diameters, enables unique opportunity for the creation of multi-functional in situ sensing capability. They demonstrated that the percolating networks of CNTs are remarkably sensitive to the onset of matrix-dominated failure and can detect the progression of damage.

The dispersion of carbon powder to the matrix of GFRP material can be used for self-diagnosing purpose was first demonstrated by Muto et al [9]. In the same work, carbon fiber was used in the GFRP material for damage monitoring by measuring its change in electrical resistance. The latter hybrid composite material was not as successive damage monitoring, when compared to GFRP material. The idea for damage monitoring of non-conductive composites via a conductive fiber was born; nevertheless this concept had been already applied in concrete structures in skyscrapers [9].

The CNT fibers have actually the size of a human hair and offer a promise for high strength and ductility, light weight, thermally and electrically conducting structural elements at a lower cost than other nanotube forms [10]. Carbon nanotube fibers can be spun by injection of carbon nanotubes suspension through an orifice into a co-flowing stream of a coagulating solution [10,11]. This can be achieved by mixing the CNT dispersion into an aqueous solution that contains a polymer (e.g. polyvinyl alcohol (PVA)) as coagulating agent. CNT fibers are conductive matters; their extra small dimensions do not impose geometrical defects on the production of the composite.

Advantages of self-sensing compared with the use of embedded or attached devices are low cost, high durability, large sensing volume, and absence of mechanical property loss. Mechanical property loss tends to occur in the case of embedded sensors, which are much larger than the diameter of carbon fiber, thereby causing bending of the carbon fiber around an embedded sensor. Durability is particularly poor for attached devices, which can be detached. Embedded sensors also suffer from the difficulty (or impossibility) of repair. Examples of embedded or attached sensors include optical fibers and piezoelectric sensors. Self-sensing has received less attention than the use of embedded or attached devices. This is due to the scientific challenge of developing self-sensing structural materials. Although much attention has been given to the mechanical properties and durability, relatively little attention has been directed to the sensing behaviour, which relates to the electrical behaviour.

In the present work, CNT fibers will be embedded to GFRP specimens in order seek simultaneously the material's response to mechanical load and its sensing capability by means of electrical resistance change in the CNT fiber. Various incremental loading–unloading steps had been applied to the manufactured specimens in tension as well as in compression. This aims to establish a direct correlation between the mechanical stress and the electrical resistance change of the CNT fiber. Investigation will be made to seek whether this correlation changes with regard to the applied mechanical loads.

2. MATERIAL MANUFACTURING

The materials used for the manufacture of the flat composite material plates with embedded carbon nanotube fibers were (a) multi-wall carbon nanotube (CNT) fibers prepared using a coagulation process, (b) epoxy resin Araldite LY564/hardener Aradur 2954 (ratio 100:35 parts by weight) and (c) glass fiber fabric PW, Style 6781 (S2-glass).

2.1. CARBON NANOTUBE FIBER

Carbon nanotube was produced with the electric-arc technique .This technique produces MWNTs in the form of bundles of a few nanotubes, along with a certain fraction of carbon impurities and catalysts. This material was sonicated in aqueous solutions of sodium dodecyl sulfate (SDS), a surfactant that adsorbs at the surface of the nanotube bundles.

At low surfactant concentrations, large and dense clusters of the initial material were still found after sonication. The amount of surfactant was too low to produce an efficient coating and induce electrostatic repulsions that could counterbalance Vander Waals attractions.

At higher SDS concentrations, black and apparently homogeneous suspensions were obtained. These suspensions did not coarsen or phase-separate macroscopically over several weeks. However, as revealed by opticalmicroscopy, dielectric measurements, and electron microscopy of freeze-fractured samples, these systems can in fact exhibit distinct phases.

At intermediate concentrations of SDS, SWNTs were homogeneously dispersed and formed a single phase. The viscosity of these systems was almost that of pure water. In this regime, the electrostatic repulsion provided by adsorbed surfactants stabilized the nanotubes against Vander Waals attraction.

Vander Waals-induced aggregation at low SDS concentration and depletion-induced aggregation at high SDS concentration, delimit an intermediate domain of homogeneously dispersed nanotubes. This domain of the phase diagram exhibits an optimum at about 0.35 wt% in nanotubes and 1.0 wt% in SDS. Subsequent processing steps were optimized at that composition because it corresponds to the maximum amount of SWNTs for which we could obtain homogeneous dispersions.

SDS-CNT was dispersed in water at a weight fraction of 0.9 wt%. The diameter of the tubes is about 10 nm. They contain catalytic iron nanoparticles supported by alumina particles. The total weight fraction of impurities is about 15 wt%. The nanotubes were purified by the following treatment: 9 wt% of MWNTs was added to a 15 wt% sulfuric acid solution. After 5 h under reflux at T = 105 ºC, the MWNTs were washed with deionized water, filtered and kept in water at a weight fraction of 10 wt%. Thermal gravimetric analyses performed with a Setaram TAG 16 instrument showed that the weight fraction of iron particles was reduced down to about

3 wt% after purification. PVA polymer had a molecular weight of 195,000 g/mol and a hydrolysis ratio of 98%. 5 wt% of the polymer dissolved in distilled water.

The CNT fiber manufacturing process consists in injecting carbon nanotube dispersion into the co-flowing stream of a coagulating polyvinyl alcohol solution. The present fibers were made in a rotating bath with the injection of the nanotube dispersion tangential to the rotation of the PVA container.

It was injected through a conical spinneret which has a diameter of 300 μm at the tip. The injection rate of the nanotube dispersion was 50 ml/ h. The spinneret was located at two centimeters from the rotation axis of the PVA container. The latter was rotated at 100 rpm to provide a co-flowing stream. The nanotubes coagulate when they met the PVA solution and formed a gel fiber. These fibers are extracted from the coagulating bath and dried vertically. The resultant systems consist in composite PVA-nanotube fibers with a fraction of carbon nanotubes of about 15 wt%. This fraction is deduced from TGA measurements performed with a Setaram TAG 16 instrument under argon flow at a heating rate of 5 ºC/min.

The CNT fiber can be washed and rinsed several times with pure water so that PVA and SDS desorbs. They can also be dried when deposited onto flat substrates. A weaker optical anisotropy was still observed in clean and dry ribbons. In spite of structural modifications arising from the drying, scanning electron microscopy of dried ribbons revealed a preferential orientation of the nanotubes along the ribbon's main axis.

Nanotube bundles and a significant amount of spherical impurities were observed. These common impurities come from the synthesis process and are mostly composed of carbon. In order to make systems that are more compact, rinsed ribbons can be suspended in air with two extremities supported on solid substrates. Capillary forces caused the water to be expelled, and the ribbon collapsed into a dense fiber with a radius of a few micrometers when dry. On the basis of the same principle, fibers several tens of centimeters long can be directly made by slowly pulling ribbons out of water.

2.2. COMPOSITE PLATES WITH EMBEDDED CNT FIBERS

Vacuum infusion method had been used to manufacture the plates of the material. Appropriate bagging material was placed, vacuum was then applied and the infusion of the resin followed. The manufactured plate was thereafter cured for 2 h at 60ºC followed by a 4 h at 120ºC post cure, as recommended by the resin manufacturer's data sheet. For the manufacturing of the plate with the CNT fibers the following process was followed. 10 plies of fabric, oriented at 0º/90º had been cut at the required dimensions (300 * 300 mm). The first 9 plies were laid and the wrap faces were alternated upwards and downwards during the lay-up, resulting in a cross-ply balanced and symmetric laminate. The CNT fibers were placed between the 9th and last ply. In total six CNT fibers were used per manufactured composite plate, this permitted the manufacturing of six testing specimens with one embedded fiber per specimen. Some contact spray adhesive was used in order to keep the CNT fibers in place while laying up the final ply.

CNT fibers were placed in such a way that they were in the middle of each testing specimen to be cut. In the distance of 50 mm (the measuring distance for the CNT fibers) two marks were covered with silver paste (conductive epoxy) and finally the

tenth ply was placed on top to complete the lay-up.

The marks covered with silver paste served to create a means of ‘‘connector” to the material’s surface, where the cables will be placed for the recording of the resistance measurements during testing. Small quantities of silver paste had been also used in the outer surface of the tenth layer of the fabrics and above the marks made in the previous layer. Small quantities were used such as not to impregnate the fabric and produce any large artificial defects on the material that would decrease its mechanical performance. The silver paste was allowed to fully cure for 24 h at room temperature.

The specimens with the CNT fiber had been cut from the material plates according to the ASTM D3039 specification and edge polished. The dimensions of the testing specimens were width * length = 25 mm * 250 mm. At the two marks of each specimen covered with silver paste, two cable connectors had been added again with silver paste in order to attach the multimeter for the resistance measurements.

3. EXPERIMENTAL PROCEDURE

Tensile test was conducted and the potential for electrical conductivity measurements for structural health monitoring was evaluated. A servo-hydraulic Instron 100 kN testing machine had been used to record the force and displacement data, while a 50 mm extensometer was attached to record axial strain data of the coupons. Additionally an Agilent multimeter was used to record in situ the electrical resistance data of the specimen’s embedded CNT fiber during mechanical loading. A DC voltage of 10 V was applied to cables connected to the CNT fiber of the specimens. The current was measured and the resistance was calculated from these values. The resistance measurements were performed in a two-point measurement set-up in the longitudinal direction. Data acquisition of 1 Hz was used for the resistance measurements and stored simultaneously in the P/C of the testing machine. A rubber mat was placed between the specimen and the metal grip of the test machine in order to insulate the specimen from the test machine. As the investigated material was the non-conductive GFRP material, no extra insulation was needed to record the electric resistance of the CNT fiber.

4. RESULTS AND DISCUSSION

4.1. TENSILE TESTS

The results for the various incremental loading–unloading loops in tensile testing, Four incremental loading–unloading steps had been made; they corresponded to the 20%, 35%, 45% and 100% of the fracture stress of the coupon, respectively. In the figure, the mechanical stress variation as well as the CNT fiber’s electrical resistance $\Delta R/R_0$ variation can be seen. After the three loading–unloading steps, the $\Delta R/R_0$ measurements of the fourth loading seems to follow the same growth curve. Fig. 1a shows the results of the direct correlation between gross mechanical stress and $\Delta R/R_0$ values. Note that the nominal strain instead of the nominal stress could also be used for such a correlation, since they are linear connected via the modulus of elasticity E. Mechanical stress had been preferred since it is the material property that is widely used in the aeronautical design office. All four loading cases can be fitted by means of a parabolic curve but in the present case an exponentially growth curve fitting provided better correlation

$$y = A \cdot e^{x/t} \quad (1)$$

The calculations of the exponential growth parameters A and t for the various loading cases can be found. After the third loading up to 45% of fracture stress, the fourth loading till fracture seems not to follow the same exponential curve. Worth noting is also that the resistance of the CNT fiber did not changed with the application of the loops and remained constant.

The loadings of another specimen aimed to increase gradually the percentage of the applied mechanical stress. Five incremental loading–unloading steps had been made and the test results can be graphically depicted in Fig. 1b. The mechanical loadings up to the 200 MPa (36% of fracture stress) or $\Delta R/R_0 = 1.5\%$ or approximate strain of 1%, showed that the resistance change measurements followed almost the same exponential curve. By applying the higher loading–unloading step up to the 60% of fracture stress, the exponential correlation between stress and $\Delta R/R_0$ ratio alters after the applied stress exceeded approximately the value of 220 MPa. This can be interpreted in both ways: either the material is 'damaged' or the CNT fiber is 'damaged'. The possibility of the damaged fiber cannot be excluded, however it is very unlikely to happen since the maximum mechanical strain of the CNT fibers exceed 200% and the current maximum applied strain is of the order of 1%. The possibility of the damaged material is also very realistic, since usually the damage in such loading cases is mainly the matrix cracking and debonding of the reinforcing fibers. The damage occurred on the third loading step (up to 36%). In the previous specimen no shift in the correlation was observed after the third step (up to 45%). Therefore the initial damage that shifts the $\Delta R/R_0$ ratio of the CNT fiber occurs between the 36% and 45% of the material's fracture stress. The additional loadings had the same impact; the exponential growth curves are again more shifted. All experimental curves in Fig. 2 were fitted by exponential growth curves of Eq. (1).

More loading–unloading steps had been performed to another specimen up to its final fractur. After the first three loading–unloading steps, the electrical resistance of the material remained the same (655 kΩ). An electrical resistance hysteresis was formed in the third loading; the loading and unloading branch can be clearly seen in the figure. After the unloading of the third step, a residual resistance was measured (658 kΩ), which can be interpreted as possible damage in the material or in the fiber. All loadings at higher stress level showed similar electrical behavior; an electrical resistance hysteresis was noticed as well as incremental residual resistance after every unloading step.

The residual electrical resistance of the CNT fiber after every incremental loading–unloading step might be attributed to the nature of the manufactured fiber. As the elastic regime limit of the CNT fiber corresponds to strain of the order of magnitude of 1–1.25%, it is eminent that there exists no accumulating damage during the loading–unloading step of the fiber below these threshold values. Hence, any observed residual resistance when the composite is loaded below these values can be directly attributed to damage of the composite material. It is not clear whether the residual resistance of the fiber for higher loadings is attributed to damage in the composite material or in the fiber. Further work is needed to confirm this hypothesis and is a matter of a running investigation.

ISSN 2348 – 7968

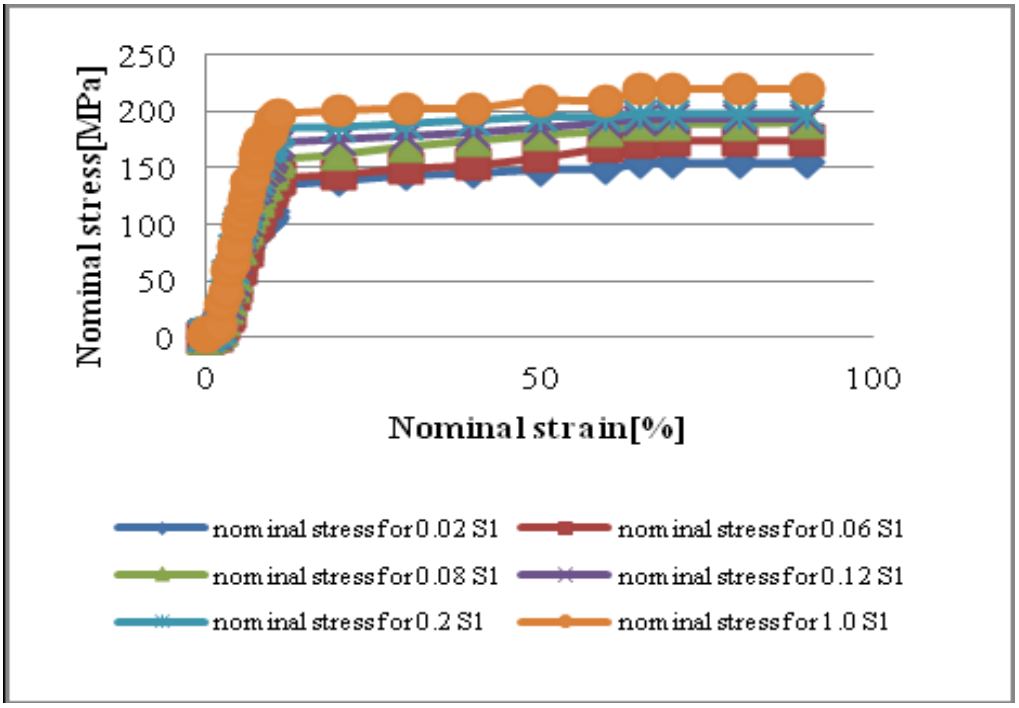

Fig.1. Typical mechanical response of the PVA-CNT fibers at 0° direction with different solvent weight ratio

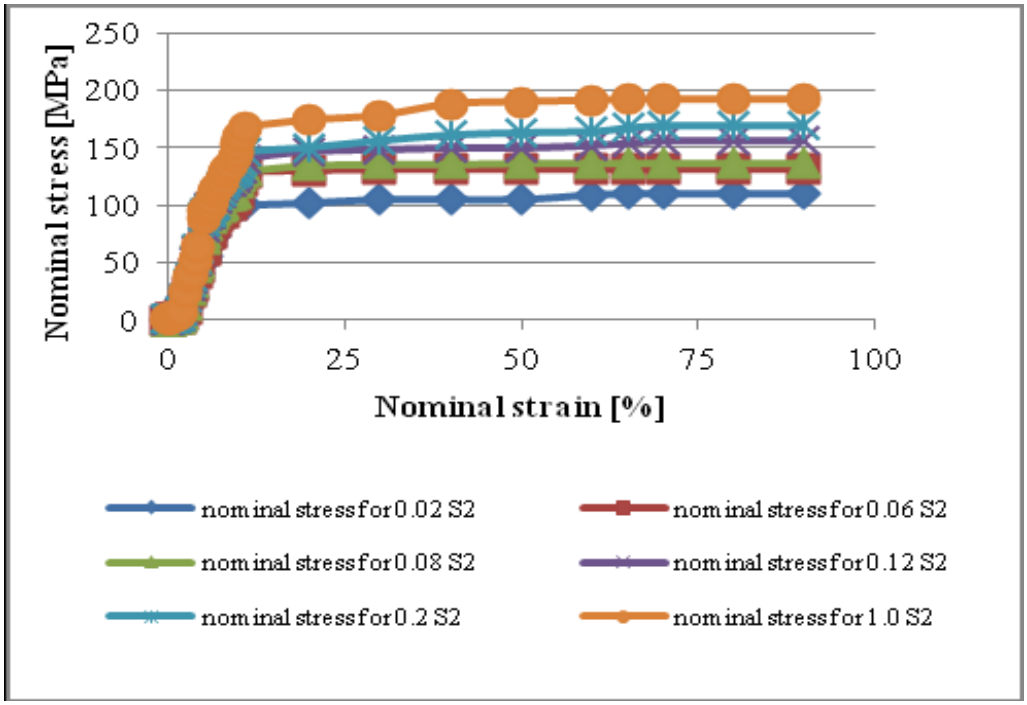

ISSN 2348 – 7968

Fig.2. Typical mechanical response of the PVA-CNT fibers at 45° direction with different solvent weight ratio

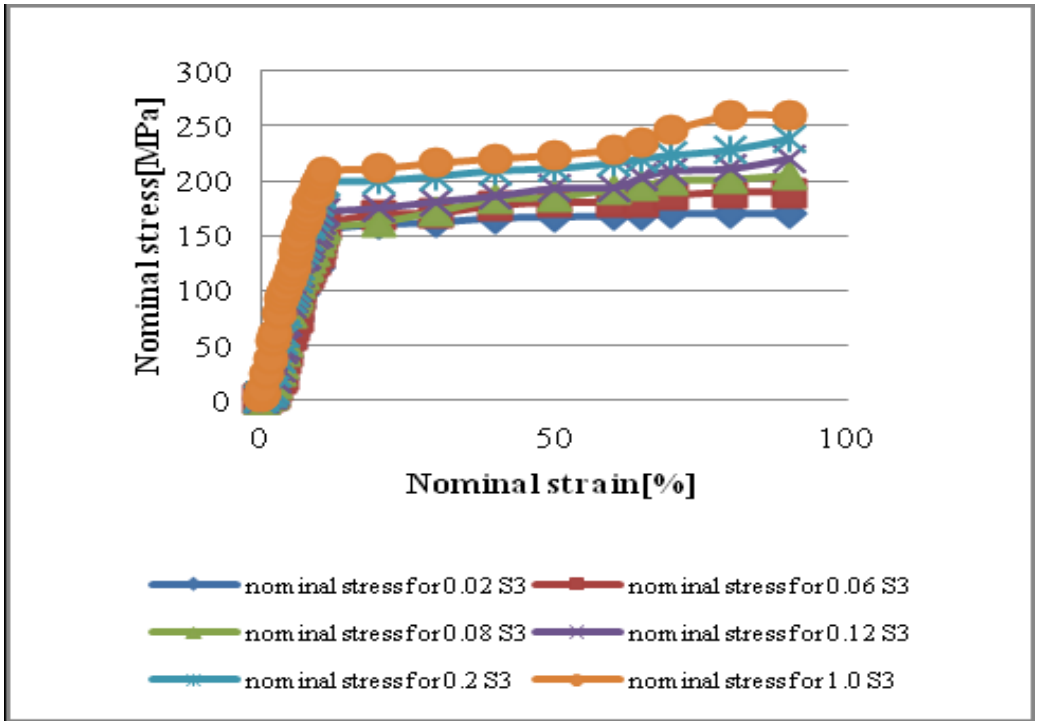

Fig.3. Typical mechanical response of the PVA-CNT fibers at 90° direction with different solvent weight ratio

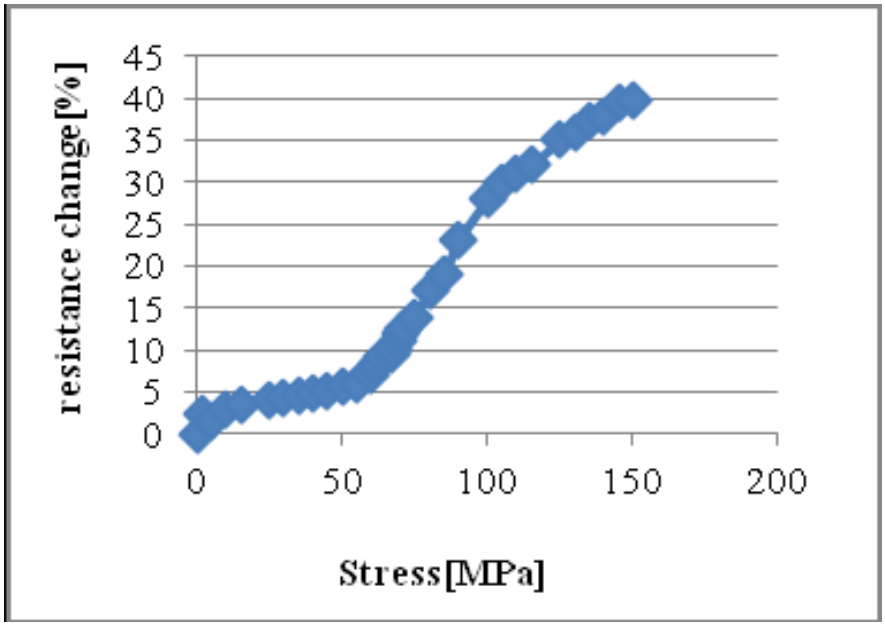

Fig.4. Typical Electrical response of the PVA-CNT fibers at 0° direction

ISSN 2348 – 7968

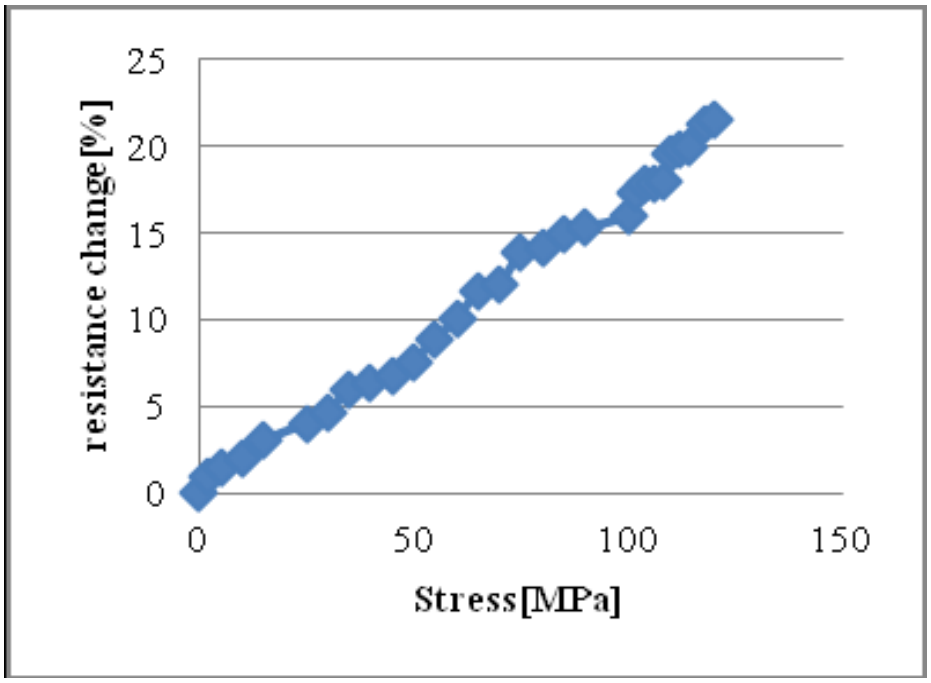

Fig.5. Typical Electrical response of the PVA-CNT fibers at 45° direction

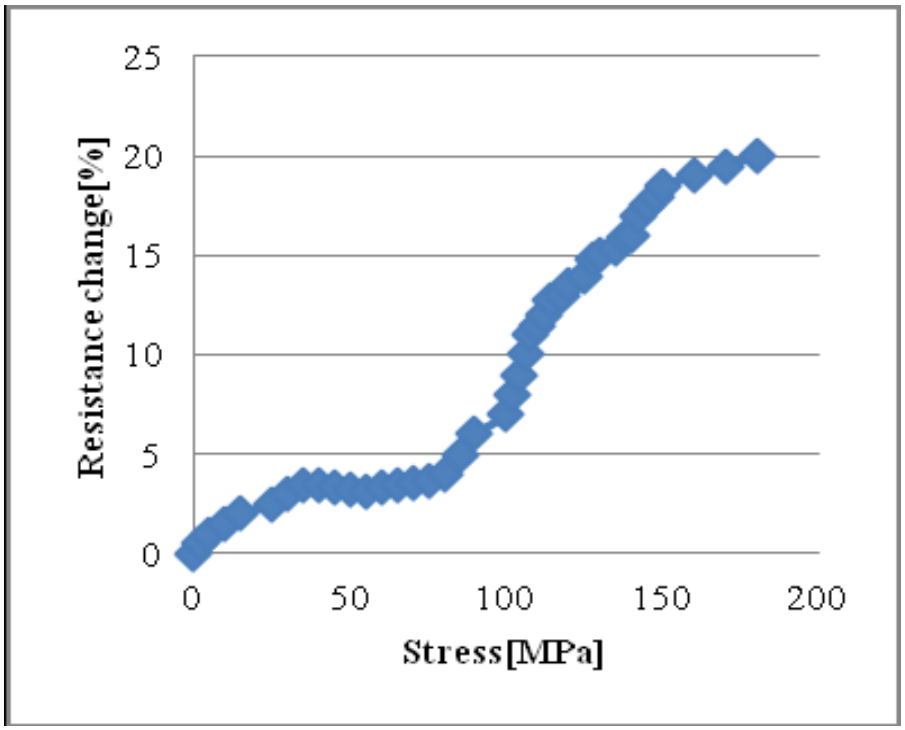

Fig.6. Typical Electrical response of the PVA-CNT fibers at 90° direction.

ISSN 2348 – 7968

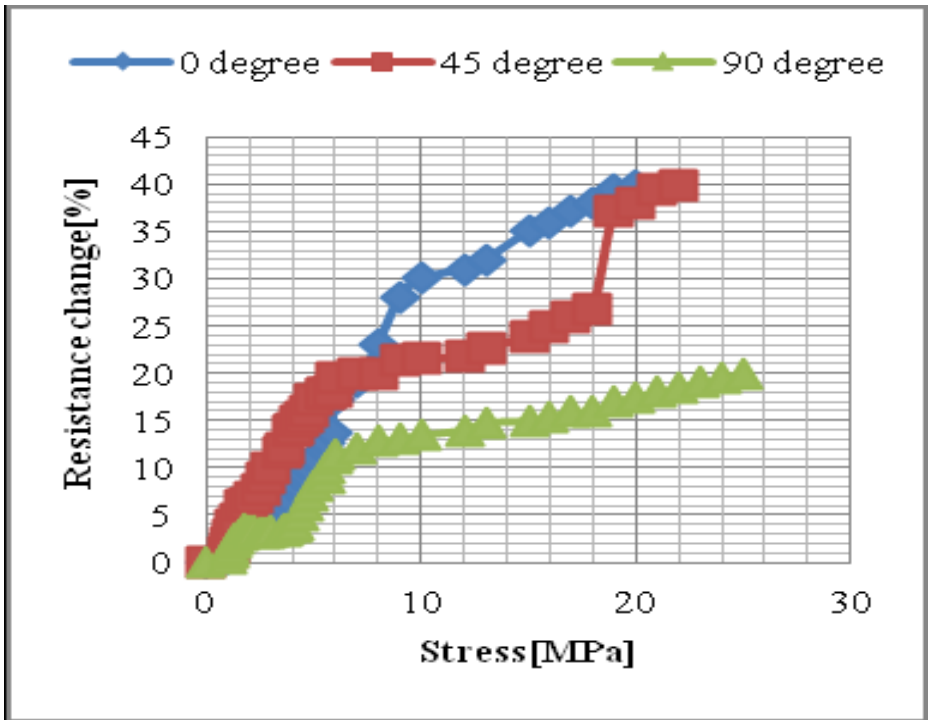

Fig.7. Comparison between the electrical responses of the corresponding direction of the PVA-CNT fibers sensor.

5. CONCLUSIONS

Glass fiber reinforced polymer (GFRP) coupons with embedded carbon nanotube (CNT) fiber had been manufactured at the laboratory for structural health monitoring via electrical resistance measurement of the CNT fiber. The following conclusions were obtained:

CNT fiber has unquestionable advantages for sensing and damage monitoring of non-conductive composites, when compared to the competitors, e.g. the embedded carbon fibers and modified (doped) conductive matrix.

The manufactured GFRP coupons with embedded CNT fibers presented the same tensile mechanical properties with the respective coupons without the CNT fiber and hence the addition of the fiber did not decrease its tensile mechanical performance.

Various incrementally tensile loading–unloading steps had been applied to different coupons with embedded CNT fibers. The applied mechanical stress of the coupon and the electrical resistance of the CNT fiber were correlated for different tensile loading cases. These parameters can be well fitted by means of a parabolic or an exponential growth curve.

By increasing the applied loading step above the level of nominal strain of 1.25% or nominal stress 220 MPa (which corresponds to almost 45% of fracture stress of the material) the correlation between stress and electrical resistance alters. Residual electrical measurements of the CNT fiber were observed; they could be

attributed to possible damage of the CNT fiber.

The above results could be used in conjunction to the coupon's accumulating damage as calculated by the decrease of the normalized modulus of elasticity E of the composite.

As the aircraft fuselage and wings skin materials are designed for tensile stresses of the order of 100 MPa (<220 MPa), as a first assessment, the electrical measurements of the CNT fiber could be used in such materials to point out whether damage due to malfunction or an overload during service has been occurred. This, of course, will produce material damage, and will definitely shift the mechanical stress – $\Delta R/R_0$ measurements.

REFERENCES

[1] S. Kaddour, F. A. R. AI-Salehi, S. T. S. A1-Hassani (1994), Electrical resistance measurement technique For detecting failure In CFRP Materials At High Strain Rates, Composites Science and Technology 51 377-385

[2] Dae-Cheol Seo, Jung-Ju Lee (1999), Damage detection of CFRP laminates using electrical resistance measurement and neural network, Composite Structures 47 525-530

[3] J.C. Abrya, S. Bochard, A. Chateauminois (1999), M. Salvia, G. Giraud, In situ detection of damage in CFRP laminates by electrical resistance measurements, Composites Science and Technology 59 925-935

[4] J.C.Abry, Y.K. Choi, A.Chateauminois, B.Dalloz, G.Giraud, M.Salvia (2001), In situ monitoring of damage in CFRP laminates by means of AC and DC measurements, Composites Science and Technology 61 855-864

[5] M.Kupke, K.Schulte, R.Schuler (2001), Non destructive testing of FRP by d.c and a.c. electrical methods, Composites Science and Technology 61 837-847

[6] Akira Todoroki, Yuuki Tanaka (2002), Delamination identification of cross-ply graphite/epoxy composite beams using electric resistance change method, Composites Science and Technology 62 629-639

[7] Akira Todoroki, Kazuomi Omagari, Yoshinobu Shimamura, Hideo Kobayashi (2006), Matrix crack detection of CFRP using electrical resistance change with integrated surface probes, Composites Science and Technology 66 1539-1545

[8] Lars Boger, Malte H.G. Wichmann, Leif Ole Meyer, Karl Schulte (2008), Load and health monitoring in glass fibre reinforced composites with an electrically conductive nanocomposite epoxy matrix, Composites Science and Technology 68 1886-1894

[9] Brigitte Vigolo, Alain Penicaud, Claude Coulon, Cedric Sauder, Rene Pailler, Catherine Journet, Patrick Bernier, Philippe Poulin (2000), Macroscopic Fibers and Ribbons of Oriented Carbon Nanotubes, Science 290:1331-4.

[10] Philippe Poulin , Brigitte Vigolo, Pascale Launois (2002), Films and fibers of oriented single wall nanotubes, Carbon 40 1741-1749

[11] N.D. Alexopoulos, C. Bartholome, P. Poulin, Z. Marioli-Riga (2010), Structural health monitoring of glass fiber reinforced composites using embedded carbon nanotube (CNT) fibers, Composites Science and Technology 70 260-271

[12] N.D. Alexopoulos, C. Bartholome, P. Poulin, Z. Marioli-Riga (2010), Damage detection of glass fiber reinforced composites using embedded PVA–carbon nanotube (CNT) fibers, Composites Science and Technology 70 1733–1741

[13] E.T. Thostenson, T.W. Chou (2006), Carbon nanotube networks: sensing of distributed strain and damage for life

ISSN 2348 – 7968

prediction and self healing, Advanced Mater 18:2837–41.
[14] E.T. Thostenson, T.W. Chou (2008), Real-time in situ sensing of damage evolution in advanced fiber composites using carbon nanotube networks, Nanotechnology 19:215713.